CRYSTALLOGRAPHIC ANALYSIS OF THE CATALYTIC MECHANISM OF HALOALKANE DEHALOGENASE

Verschueren, Koen H.G.; Seljée, Frank; Rozeboom, Henriette; Kalk, Kor H.; Dijkstra, Bauke W.

Published in:
Nature

DOI:
10.1038/363693a0

66. Zhou, P., Dong, Z. H., Rao, A. M. & Eklund, P. C. *Science*, submitted.
67. Yeretzian, C., Hansen, K., Diederich, F. & Whetten, R. L. Nature **359,** 44–46 (1992).
68. Wood, J. M., *et al. J. Am. chem. Soc.* **113,** 5907–5908 (1991).
69. Kalsbeck W. A. & Thorp, H. W. *J. electroanal. Chem.* **314,** 363–365 (1991).
70. Diederich, F. *et al. Science* **252,** 548–549 (1991).
71. Taylor, R. *et al. J. chem. Soc. chem. Commun.*, 667–668 (1992).
72. Tuinman, A. A., Mukherjee, P., Adcock, J. L., Hettich, R. L. & Compton, R. N. *J. phys. Chem.* **96,** 7584–7589 (1992).
73. Creegan, K. M. *et al. J. Am. chem. Soc.* **114,** 1103–1105 (1992).
74. Elemes, Y. *et al. Angew. Chem. int. Edn. Engl.* **31,** 351–353 (1992).
75. Arbogast, J. W. *et al. J. Phys. Chem.* **95,** 11–12 (1991).
76. Taylor, R. *et al. J. chem. Soc. chem. Commun.* 875–878 (1993).
77. Raghavachari, K. *Chem. Phys. Lett.* **195,** 221–224 (1992).
78. Raghavachari, K. & Rohlfing, C. M. *Chem. Phys. Lett.* **97,** 495–498 (1992).
79. Suzuki, T., Li, Q., Khemani, K. C., Wudl, F. & Almarsson, Ö. *Science* **254,** 1186–1188 (1991).
80. Suzuki, T., Li, Q., Khemani, K. C., Wudl, F. & Almarsson, Ö. *J. Am. chem. Soc.* **114,** 7300–7301 (1992).
81. Suzuki, T., Li, Q., Khemani, K. C. & Wudl. F. *J. Am. chem. Soc.*, 7301–7302 (1992).
82. Vasella, A., Uhlmann, P., Waldruff, C. A. A., Diederich, F. & Thilgen, C. *Angew Chem. int. Edn Engl.* **31,** 1388–1390 (1992).
83. Fagan, P. J., Calabrese, J. C. & Malone, B. *Accts chem. Res.* **25,** 134–142 (1992).
84. Koefod, R. S., Hudgens, M. F. & Shapley, J. R. *J. Am. chem. Soc.* **113,** 8957–8958 (1991).
85. Balch, A. L., Lee, J. W., Noll, B. C. & Olmstead, M. M. *J. Am. chem. Soc.* **114,** 10984–10985 (1992).
86. Balch, A. L., Lee, J. W. & Olmstead, M. M. *Angew. Chem. int. Edn Engl.* **31,** 1356 (1992).
87. Hawkins, J. M., *et al. J. org. Chem.* **55,** 6250–6252 (1990).
88. Tebbe, F. N., *et al. J. Am. chem. Soc.* **113,** 9900–9901 (1991).
89. Olah, G. A., *et al. J. Am. chem. Soc.* **113,** 9385–9387 (1991).
90. Birkett, P. R., Hitchcock, P. W., Kroto, H. W., Taylor, R. & Walton, D. R. M. *Nature* **357,** 479–481 (1992).
91. Tebbe. F. N. *et al. Science* **256,** 822–825 (1992).
92. Birkett, P. R. *et al. J. chem. Soc. chem. Commun.* (in press).
93. Holloway, J. H. *et al. J. chem. Soc. chem. Commun.*, 966–969 (1991).
94. Selig, H. *et al. J. Am. chem. Soc.* **113,** 5475–5476 (1991).
95. Kniaz, K. *et al. J. Am. chem. Soc.* (submitted).
96. March, J. *Advanced Organic Chemistry*, 707–708 (Wiley, Chichester, 1992).
97. Wudl, F. *et al. Am. chem. Soc. Symp. Series* **481,** 161–175 (1991).
98. Hirsch, A., Li, Q. & Wudl, F. *Angew. Chem. int. Edn Engl.* **30,** 1309–1310 (1992).
99. Miller, G. P., Millar, J. M., Liang, B., Uldrich, S. & Johnston, J. E. *J. chem. Soc. chem. Commun.* 897–899 (1993).
100. Hoke, S. H. *et al. Rapid Commun. Mass Spectrom.* **5,** 472–474 (1991).
101. Chiang, L. Y. *et al. J. chem. Soc. chem. Commun.*, 1791–1793 (1992).
102. Chiang. L. Y. Upasani, R. B. & Swirczewski, J. W. *J. Am. chem. Soc.* **114,** 10154–10157 (1992).
103. Krusic, P. J. *et al. J. Am. chem. Soc.* **113,** 6274–6275 (1991).
104. Morton, J. R., Preston, K. F., Krusic, P. J. & Wasserman, E. *J. chem. Soc. Perkin Trans.* 2, 1425–1429 (1992).
105. Krusic, P. J., Wasserman, E., Keizer, P. N., Morton, J. R. & Preston, K. F. *Science* **254,** 1183–1185 (1991).
106. Taylor, R. *Electrophilic Aromatic Substitution*, 15–18 (Wiley, Chichester, 1989).
107. Morton, J. R., Preston, K. F., Krusic, P. J., Hill, S. A. & Wasserman, E. *J. phys. Chem.* **96,** 3576–3578 (1992); *J. Am. chem. Soc.* **114,** 5454–5456 (1992).
108. Keizer, P. N., Morton, J. R. & Preston, K. F. *chem. Soc. chem. Commun.*, 1259–1261 (1992).
109. Taylor, R. *et al. Nature* **355,** 27–28 (1992).
110. Amato, I. *Science* **254,** 30–31 (1991).
111. Loy, D. A. & Assink, R. A. *J. Am. chem. Soc.* **114,** 3977–3978 (1992).
112. Samulski, E. T. *et al. Chem. Mater.* **4,** 1153–1157 (1992).
113. Nagashima, H. *et al. J. chem. Soc. chem. Commun.*, 377–379 (1992).
114. Tutt, L. W. & Kost, A. *Nature* **356,** 225–226 (1992).
115. Wang, Y. *Nature* **356,** 585–587 (1992).
116. Loutfy, R. O. & Withers, J. C. Abstract 2145, *Electrochem. Soc. Meeting*, Hawaii (1993).

Crystallographic analysis of the catalytic mechanism of haloalkane dehalogenase

Koen H. G. Verschueren, Frank Seljée, Henriëtte J. Rozeboom, Kor H. Kalk & Bauke W. Dijkstra*

BIOSON Research Institute and Laboratory of Biophysical Chemistry, University of Groningen, Nijenborgh 4, 9747 AG Groningen, The Netherlands

Crystal structures of haloalkane dehalogenase were determined in the presence of the substrate 1,2-dichloroethane. At pH 5 and 4 °C, substrate is bound in the active site without being converted; warming to room temperature causes the substrate's carbon–chlorine bond to be broken, producing a chloride ion with concomitant alkylation of the active-site residue Asp_{124}. At pH 6 and room temperature the alkylated enzyme is hydrolysed by a water molecule activated by the His_{289}–Asp_{260} pair in the active site. These results show that catalysis by the dehalogenase proceeds by a two-step mechanism involving an ester intermediate covalently bound at Asp_{124}.

THE nitrogen-fixing hydrogen bacterium *Xanthobacter autotrophicus* GJ10 can grow on a medium containing 1,2-dichloroethane or 2-chloroethanol as the sole carbon and energy source[1]. The organism is being investigated for application in the clean up of environmentally harmful halogenated compounds, some of which are industrially produced in large amounts for use as cleaning agents, pesticides and solvents. The first step in the degradation of these compounds by the bacterium is catalysed by haloalkane dehalogenase[1], an enzyme having an M_r of 36K and a known nucleotide and amino-acid sequence[2,3]. It converts 1-haloalkanes into primary alcohols and a halide ion by hydrolytic cleavage of the carbon–halogen bond, with water as a co-substrate and without any need for oxygen or cofactors[2], at an optimal pH of 8.2. The crystal structure of the enzyme has been determined at 2.4 Å resolution[4] and refined to 1.9 Å (ref. 27). The putative active site is located between the two domains of the protein in an internal, predominantly hydrophobic cavity. Asp_{124}, His_{289} and Asp_{260}, which are located in this cavity, have been proposed to be the catalytic residues. They form a catalytic triad, with the triad residues occurring at the same topological positions as in other members of the α/β hydrolase-fold family[5], despite any clear sequence homology. To this family also belong acetylcholinesterase from *Torpedo californica*[6], dienelactone hydrolase from *Pseudomonas* sp. B13 (ref. 7), carboxypeptidase II from wheat[8,9] and lipases[10]. All members of this family have a similar core formed by an α/β sheet of eight β-strands connected by α-helices. In addition, they all have a small pocket near the amide nitrogen of the residue following the nucleophile, which could be the oxyanion hole[5], indicating that they may share a similar reaction mechanism. The proposed nucleophilic residue for the dehalogenase (Asp_{124}) is quite different from that of the other enzymes (Ser or Cys), however, and the bond to be

* To whom correspondence should be addressed.

hydrolysed (carbon–halogen) is rather different from the ester or amide bond cleaved by the other enzymes. From the architecture of the active site of dehalogenase, there are two possible reaction mechanisms for hydrolytic dehalogenation: the first could be a nucleophilic substitution by the carboxylate anion of Asp_{124}, resulting in a covalently bound intermediate ester that might subsequently be hydrolysed by a water molecule, activated by His_{289} as base (Fig. 1*a*)[4,11]; the second possibility is a general base catalysis with a water molecule activated by His_{289} (ref. 11; Fig. 1*b*).

To discriminate between these two possibilities and to compare the dehalogenase catalytic mechanism with that of the other members of the α/β hydrolase-fold family, we analysed the catalytic pathway in dehalogenase as a function of pH and temperature by high-resolution X-ray crystallography. Both putative dehalogenase catalytic mechanisms require that the His_{289} side chain is mainly deprotonated at the pH of optimal activity. A crystal structure determined at pH 8.2 shows that this is indeed the case[5,27]. But at low pH, with the His_{289} side chain protonated and no longer acting as a base, according to the first mechanism the covalently bound intermediate could accumulate in the active site, whereas by the second mechanism, substrate should bind without being degraded. We therefore soaked dehalogenase crystals in mother liquor containing the substrate 1,2-dichloroethane at different pHs and temperatures. This allowed us to obtain three-dimensional structures of (1) dehalogenase with substrate bound in its active site; (2) dehalogenase with the covalently bound intermediate; (3) dehalogenase with chloride as the product of the reaction bound in the active site. From these structures we conclude that the reaction catalysed by the dehalogenase proceeds through a two-step catalytic mechanism with a covalently bound intermediate.

Substrate binding

Substrate was bound in the active site of dehalogenase by soaking crystals for three hours in mother liquor[12] with 10 mM 1,2-dichloroethane at pH 5.0 and 4 °C. A difference Fourier showed clear density in the active-site cavity in which a 1,2-dichloroethane molecule could be fitted. The final structure, refined at 2.4 Å resolution, shows that one chlorine atom of the substrate (Cl–1) is bound to the ring nitrogen atoms of Trp_{125} and Trp_{175} (Cl–N distances are 3.6 Å and 3.2 Å, respectively) (Fig. 2*a*). Cl–1 lies nearly on the intersection of the planes of the two tryptophan rings, thus maximizing the favourable interactions with the slightly positively charged hydrogen atoms of the aromatic ring nitrogens. The second chlorine atom (Cl–2) is not bound very tightly and may be flexible, interacting with the side chains of Phe_{128}, Phe_{172} and perhaps Phe_{164}. The substrate's C_1 carbon atom, which is connected to Cl–1, is near the $O_{\delta 1}$ atom of Asp_{124}, at 3.8 Å. The protein atom closest to C_2 is $C_{\gamma 2}$ of Val_{226}, at 3.3 Å; the Asp_{124} $O_{\delta 1}$ atom is at 3.6 Å. At pH 6.2 as well as under the present conditions, the Asp_{124} side chain is hydrogen-bonded to the $N_{\varepsilon 2}$ atom of His_{289} (distance is 2.6–2.7 Å). At

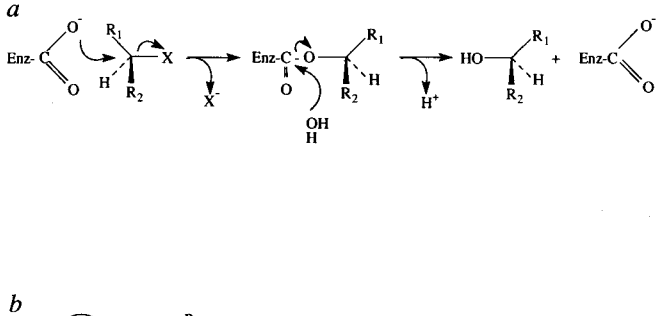

FIG. 1 *a*, *b*, Possible reaction mechanisms for the hydrolytic dehalogenation by haloalkane dehalogenase from *Xanthobacter autotrophicus* GJ10.

TABLE 1 Summary of the crystallographic analyses

	Crystal 1 pH 5.0 +10 mM substrate + cooling at 4 °C	Crystal 2 pH 5.0 +10 mM substrate +RT	Crystal 3 pH 6.2 +10 mM substrate +RT
pH	5.0	5.0	6.2
Temperature	4 °C	22 °C	22 °C
Number of crystals	1	1	1
Soaking time	3 h	24 h	96 h
Total exposure time less	48 h	48 h	48 h
Resolution range	2.39 Å	1.99 Å	2.14 Å
Space group	$P2_12_12$	$P2_12_12$	$P2_12_12$
Unit cell dimensions:			
a	94.9 Å	94.8 Å	95.0 Å
b	72.8 Å	72.8 Å	72.6 Å
c	41.4 Å	41.4 Å	41.4 Å
Total number of observations	34,590	39,634	36,467
Number of unique reflections	11,326	16,812	14,119
Number of discarded observations	2,549	1,254	1,284
R_{merge} (%)	12.44	4.06	5.74
Completeness of the data (%)	94.6	82.0	84.7
Stereochemical quality			
Number of residues	1–310	1–310	1–310
Number of solvent molecules	125	151	188
Final *R*-factor (%)	19.5	18.6	16.5
Coordinate error estimates from a σ_A plot (Read, 1986)	0.12 Å	0.15 Å	0.13 Å
R.m.s. deviations from ideality for bond lengths (Å)	0.014	0.010	0.009
bond angles	3.9°	3.0°	2.9°
Special features compared to native dehalogenase:	Substrate bound in active-site cavity	Alkyl-enzyme Chloride product	Chloride product Hydrolytic water has disappeared
	Hydrolytic water	Hydrolytic water disappears	New incoming water in cavity

RT, room temperature. The gene coding for native haloalkane dehalogenase from *Xanthobacter autotrophicus* GJ10 was cloned and overexpressed in cultures of *Escherichia coli* HB101 (ref. 3). The isolated and purified enzyme[2,3,27] gave good sized crystals grown from a 60% (w/v) saturated (at 0 °C) $(NH_4)_2SO_4$ solution buffered at pH 6.2 with 100 mM bis-Tris(bis(2-hydroxyethyl)-iminotris(hydroxymethyl)-methane), using vapour diffusion in hanging drops[12]. The space group is orthorhombic, $P2_12_12$, with unit cell dimensions $a = 94.8$ Å, $b = 72.8$ Å and $c = 41.4$ Å. Soaking of the crystals in mother liquor containing 10 mM 1,2-dichloroethane at the different pHs and temperatures had negligible effect on the size of the unit cell. X-ray intensities of the different complexes were collected with a FAST area detector (Enraf Nonius, Delft) equipped with a CAD4 κ-goniostat, with graphite monochromatized Cuκ_α radiation from an Elliot GX21 rotating anode generator as X-ray source. Data collection and reduction was done with the MADNES system[22]; profile fitting of the data was according to Kabsch[23]. Data were scaled[24] and merged using the Groningen BIOMOL crystallographic software package.

$$R_{merge} = \frac{\sum_{hkl} \sum_{refl} |I(hkl,j) - \bar{I}(hkl)|}{\sum_{hkl} \sum_{refl} |I(hkl,j)|} \times 100\%$$

where I is the observed intensity and $\bar{I}$ is the average intensity obtained from multiple observations of symmetry-related reflections.

$$R\text{-factor} = \frac{\sum ||F_{obs}| - |F_{calc}||}{\sum |F_{obs}|} \times 100\%$$

pH 8.2, the pH optimum of the dehalogenase, this hydrogen bond is lost[27] and both the Asp_{124} and His_{289} side chains have moved apart (by 0.6 Å). Assuming that the substrate position at pH 8.2 is the same as at pH 5.0, the Asp_{124} $O_{\delta 1}$ atom at pH 8.2 would be somewhat closer to the substrate's C_1 atom (at about 3.7 Å), and could perform a nucleophilic attack. There are no water molecules close to one of the substrate's carbon atoms, the nearest water molecule being at 5.7 Å from C_1. This makes a direct attack of a water molecule on the C_1 carbon atom of the substrate extremely unlikely. However, there is a water molecule (H_2O_{485} in Fig. 2*a*) present close to the Cγ atom of Asp_{124} (distance 2.8 Å), which could hydrolyse the proposed ester intermediate at Asp_{124}. This water molecule is near the $N_{\epsilon 2}$ atom of residue His_{289}, which also hydrogen-bonds with its $N_{\delta 1}$ atom to the side chain of Asp_{260}. A schematic view of the residues important for substrate binding is given in Fig. 3*a*.

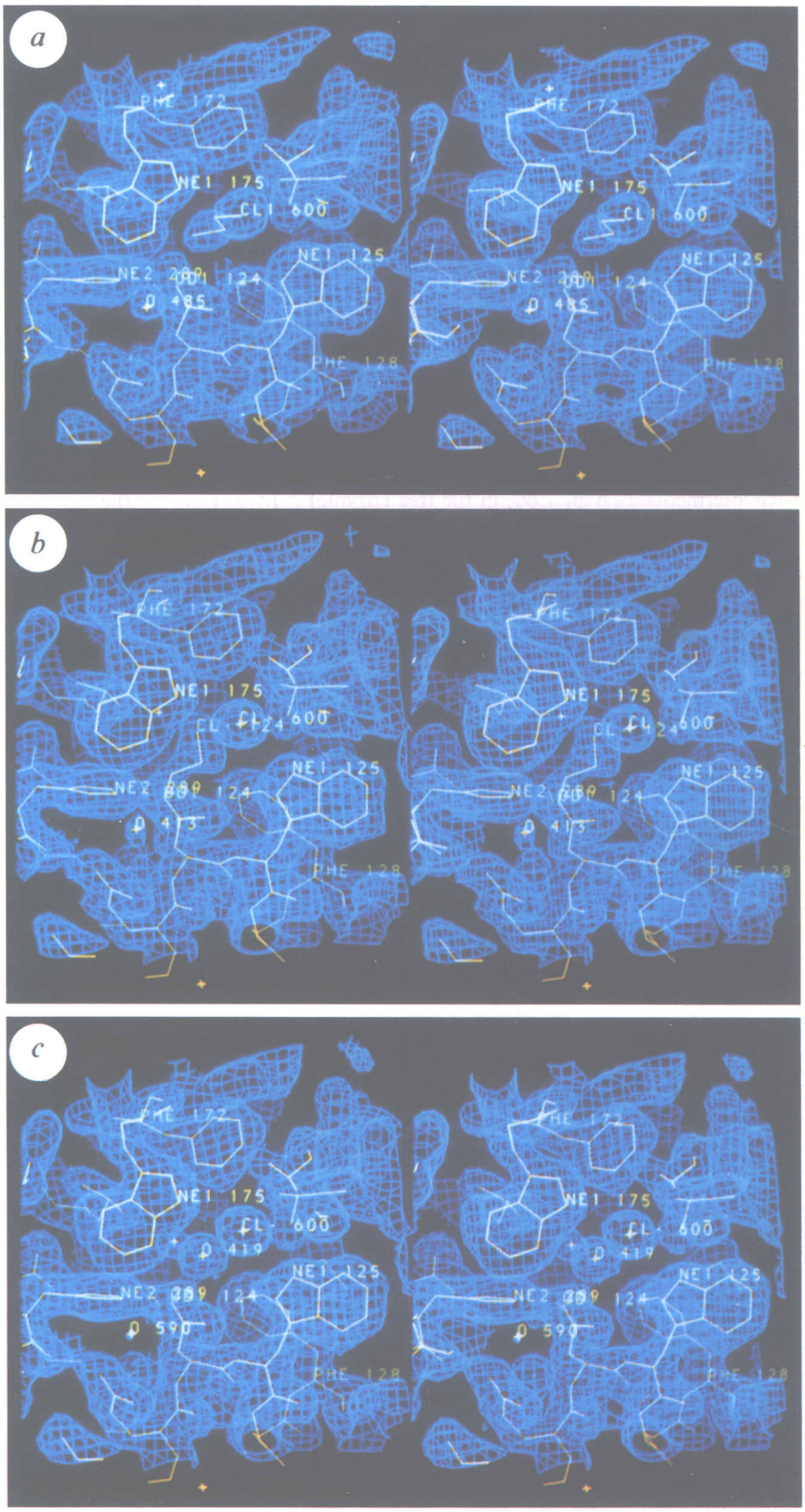

FIG. 2*a* Stereo view of the final 2.4 Å-resolution σ_A-weighted[25] $(2m|F_{obs}| - D|F_{calc}|)exp(i\alpha_{calc})$ electron density map showing a substrate molecule bound in the active site of haloalkane dehalogenase. Crystals were mounted in X-ray capillaries at 4° C and directly transferred to a FAST television area detector, where data collection was carried out at 4° C over a two-day period. The pH 6.2 structure of dehalogenase, determined at 1.9 Å resolution[27] without solvent molecules, was used as the starting model for the crystallographic refinement with the TNT program[26]. Details of the soaking procedure, data collection and the refinement statistics are given in Table 1. *b*, Stereo view of the final 2.0 Å-resolution σ_A-weighted[25] $(2m|F_{obs}| - D|F_{calc}|)exp(i\alpha_{calc})$ electron density map showing the electron density for the covalently bound intermediate of the dehalogenase. *c*, Stereo view of the final 2.14 Å-resolution σ_A-weighted[25] $(2m|F_{obs}| - D|F_{calc}|)exp(i\sigma_{calc})$ electron density map showing the electron density for the dehalogenase with chloride as a reaction product bound. The atomic coordinates have been deposited with the Brookhaven Protein Data Bank.

The alkyl-enzyme

Soaking native dehalogenase crystals for one day in 10 mM 1,2-dichloroethane at pH 5 and at room temperature caused the accumulation of a covalent intermediate in the crystal (Fig. 2*b*). Clear extra density extends from the $O_{\delta 1}$ atom of the side chain of Asp_{124}, and the covalently bound intermediate can easily be built into this density. A spherical electron density, consistent with the density for a chloride ion in an ($|F_{obs}|$(substrate) − $|F_{obs}|$(native)) difference Fourier is located between the side chains of two tryptophan residues (residues 125 and 175). This density is not connected to the density extending from the Asp_{124} side chain, indicating that the carbon–halogen bond has been cleaved, and that a chloride ion and a covalently bound intermediate have been formed. This is clear evidence for the proposed two-step mechanism, with the Asp_{124} side chain acting as the first nucleophile[4]. The chloride ion is at the same position as the Cl–1 atom in the bound substrate, and interacts with the ring nitrogen atoms of the Trp residues (at 3.5 Å and 3.2 Å from the N_η atoms of Trp_{125} and Trp_{175}, respectively). The two carbon atoms of the covalently bound substrate make van der Waals contacts with Phe_{128}, Trp_{175} and His_{289}. In contrast to the weak density observed for the Cl–2 atom in the enzyme–substrate complex, the density for Cl–2 in the alkyl–enzyme complex is unambiguous (Fig. 2*b*). Cl–2 lies in the plane of the Phe_{172} side chain and may be stabilized by interactions with the hydrogen atoms at the $C_{\delta 1}$ and $C_{\varepsilon 1}$ atoms of this residue. The Asp_{124} and His_{289} side chains have barely moved relative to their position in the enzyme–substrate complex. The carbonyl oxygen of the ester intermediate (Asp_{124} $O_{\delta 2}$ in the free enzyme) is hydrogen-bonded to the peptide nitrogen atoms of residues 56 and 125, whereas the ester oxygen atom (Asp_{124} $O_{\delta 1}$) is hydrogen-bonded to the His_{289} $N_{\varepsilon 2}$ atom. Also the water molecule close to the C_γ atom of Asp_{124} in the complex with substrate, is still present, although its electron density has decreased (H_2O_{413} in Fig. 2*b*). Assuming the temperature factor of this water to be similar to those of the surrounding atoms, its occupancy refined to about 0.4. This strongly suggests that, under our experimental conditions, this water molecule is slowly acting as the nucleophile in the second reaction step, in which the ester intermediate is hydrolysed, without being replenished. This water is completely secluded from the solvent and it is probably replenished from the active site cavity (see below). Some new electron density is already observed for an incoming water molecule near the Cl–2 atom. In agreement with the partial occupancy of the hydrolytic water, we estimate the occupancy of the covalently bound intermediate to also be about 0.4 to 0.5. Figure 3*b* gives a schematic overview of the interactions of the alkyl group with the enzyme.

After hydrolysis of the alkyl intermediate

Soaking native dehalogenase crystals for two days at room temperature in a mother liquor with 10 mM 1,2-dichloroethane at pH 6.2 results in a complex of dehalogenase with chloride as the product (Fig. 2*c*). There is no longer any density corresponding to the covalently bound intermediate, or the product 2-chloroethanol. But we still observe a spherical density consistent with a chloride ion located between the side chains of Trp_{125} and Trp_{17} (Fig. 2*c*). Also an ($|F_{obs}|$(product) − $|F_{obs}|$(native)) difference Fourier clearly discriminates this chloride ion from a solvent molecule. Thus, at pH 6.2 the crystallized enzyme has low activity. One of the products of the reaction, the 2-chloroethanol, has already left the active site cavity, but the chloride ion—the other product—is still present. In addition to the chloride ion, the active-site cavity contains two water molecules. One occupies a position near where the Cl–2 atom was situated in the covalently bound intermediate, and the other is hydrogen-bonded to the $O_{\delta 1}$ atom of the Asp_{124} side chain (Fig. 3*c*). The $O_{\delta 1}$ atom is also hydrogen-bonded to the His_{289} $N_{\varepsilon 2}$ atom, as we found in the native dehalogenase structure at pH 6.2 (refs 4, 27). To our surprise, although the density of the hydrolytic water molecule is clear near the C_γ atom of Asp_{124} in the native structure at pH 6.2 and in the enzyme–substrate complex and the alkyl-enzyme, it has almost completely disappeared in the

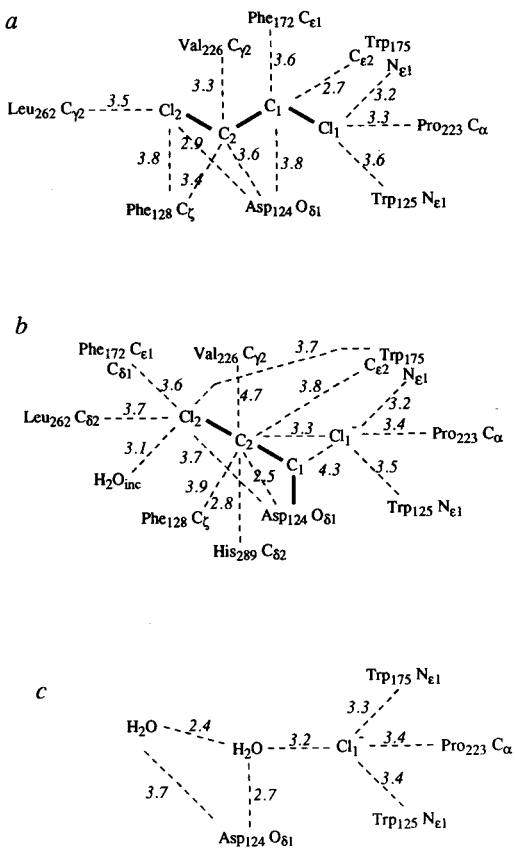

FIG. 3 Schematic view of the interactions of the active site residues of dehalogenase *a*, with the substrate, before the start of the reaction; *b*, with the alkyl intermediate and the chloride ion, during the reaction; *c*, with the chloride ion and the water molecules, after hydrolysis.

present structure (H_2O_{590} in Fig. 2*c*). This indicates that this is the water molecule essential for the hydrolysis of the covalently bound intermediate, but that it is replenished after hydrolysing the alkyl-enzyme only very slowly under the conditions applied. The water molecule most likely to replenish the hydrolytic water is the one hydrogen-bonded to the Asp_{124} side chain. Presumably at pH 6.2, the hydrogen bond between the Asp_{124} and His_{289} side chains is strong enough to limit the mobility of Asp_{124} and to restrict the accessibility to the binding site of the hydrolytic water molecule. Indeed, if the experiment is done at pH 8.2, we find that the hydrolytic water molecule has been (partly) replenished. Interestingly, in contrast to the native dehalogenase structure at

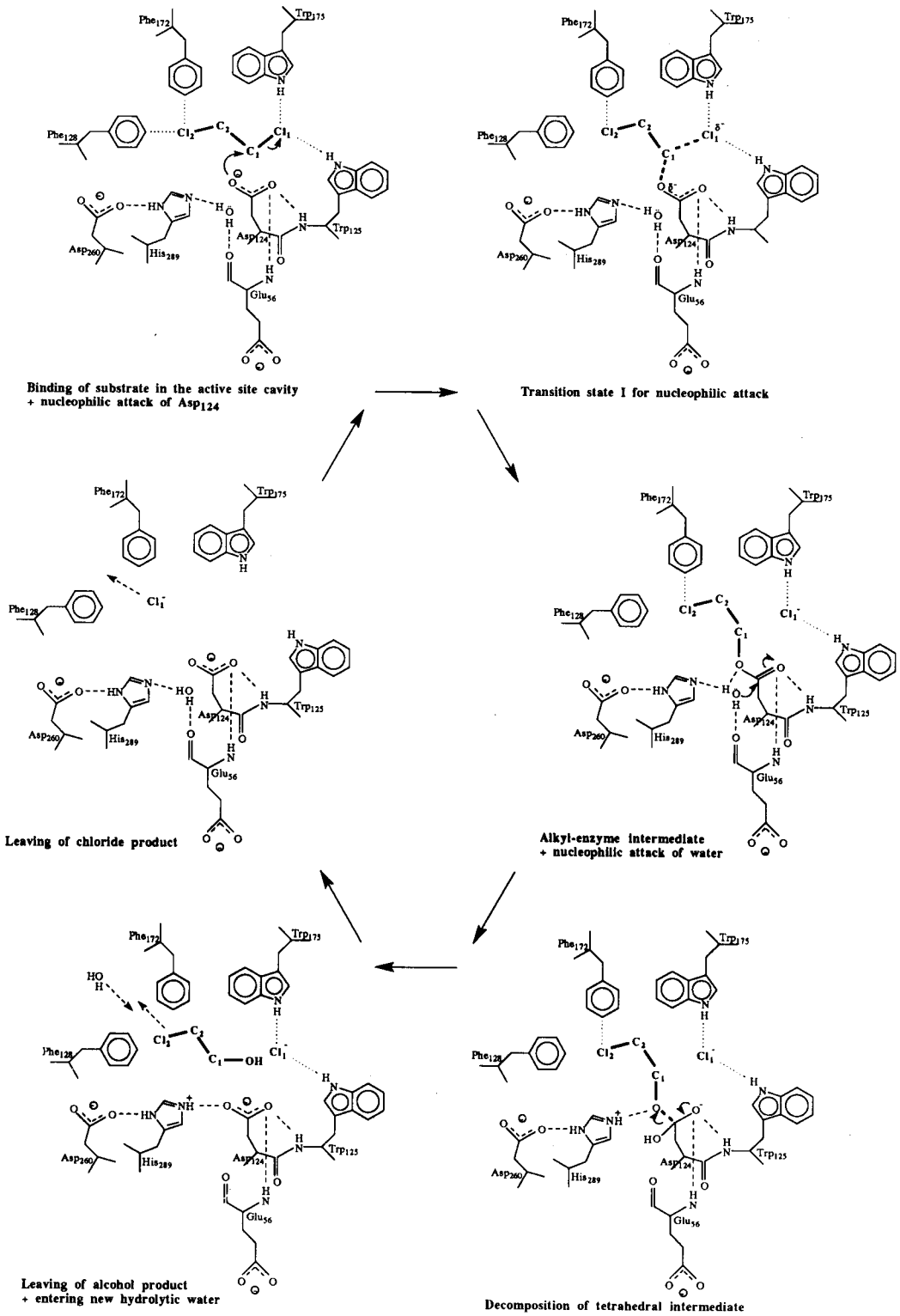

FIG. 4 Reaction mechanism at the optimal pH (pH 8.2) of haloalkane dehalogenase as deduced from the crystal structures of the native enzyme without substrate at pH 8.2 (ref. 27) and from the structures described here.

pH 8.2, in which there is no hydrogen bond between the Asp_{124} and His_{289} side chains[27], a hydrogen bond exists between Asp_{124} and His_{289} even at pH 8.2 if a chloride ion is present in the active site. This suggests that the release of chloride from the substrate increases the pK_a of the His_{289} side chain, thereby facilitating its function as a general base to activate the hydrolytic water molecule.

Discussion

By variation of pH and temperature in soaking experiments of native haloalkane dehalogenase crystals with the substrate 1,2-dichloroethane, we succeeded in trapping different stages in the enzyme's reaction pathway. The first step of the reaction, the formation of the enzyme-substrate complex, could be trapped at low pH and low temperature. Increasing the temperature resulted in the accumulation of a covalently bound intermediate, and increasing, in addition, the pH to 6.2 allowed the release of the alcohol product but left the chloride product still bound in the active site. The reaction intermediates that we observe are reasonably stable under the experimental conditions. Their lifetimes are long enough to allow collection of diffraction data sets by standard methods over two-day periods without completely being converted. The resulting structures show the intermediates in significant occupancies.

Our experiments confirm the two-step catalytic mechanism proposed earlier[4], in which Asp_{124} is the nucleophile in the first step of the reaction and a water molecule hydrolyses the covalent ester intermediate in the second step (see Fig. 4 for a summary of the reaction mechanism). In this respect they are consistent with the reaction mechanisms in other α/β hydrolase-fold enzymes, in which a covalent intermediate is also formed that is hydrolysed by a water molecule (for example, acetylcholinesterase[13] and serine carboxypeptidases[14]. But whereas in these other enzymes the same carbonyl carbon atom of the substrate molecule is attacked twice (first by the enzyme's nucleophile (Ser or Cys), and subsequently by a water molecule), in dehalogenase two different atoms are targets of nucleophilic attack; first the C_1 carbon atom of the substrate is attacked by the $O_{\delta 1}$ atom of Asp_{124} to form a covalently bound ester, and next this ester is hydrolysed by a water molecule that attacks the C_γ atom of the Asp_{124} residue. As a consequence, the dehalogenase reaction pathway proceeds through completely different transition states, each with its own stabilization. In the first step, the transition state is presumably a penta-coordinated C_1 carbon atom of the substrate, as occurs in *SN2* substitution reactions at sp3 carbon atoms, with the negative charge developing on the halogen atom stabilized by the slightly positively charged N–H atoms of the Trp_{125} and Trp_{175} side chains. This step is unique for the dehalogenase. The second reaction step proceeds through a tetrahedral intermediate at the C_γ atom of Asp_{124}. The transition states for the formation and breakdown of this tetrahedral intermediate may be stabilized by interactions with the peptide nitrogen atoms of Glu_{56} and Trp_{125}, which are in the small oxyanion pocket. The $O_{\delta 2}$ atom of Asp_{124}, which is negatively charged in the tetrahedral intermediate, hydrogen-bonds with these backbone NH groups in all the native and complexed dehalogenase structures analysed so far. All α/β-fold hydrolases have such a small pocket in common, near the amide nitrogen of the residue following the nucleophile[5]. In the wheat serine carboxypeptidase, the peptide nitrogen of Gly_{53} was suggested to be part of the oxyanion-binding site[9]. It is located at the C terminus of β-strand 3 (α/β hydrolase-fold numbering) at a position equivalent to that of Glu_{56} in dehalogenase. In addition, in dehalogenase the $O_{\delta 2}$ atom of Asp_{124} is positioned very close to the axis of helix C, at the N-terminal side of the helix. Thus, the negative charge developing on the $O_{\delta 2}$ atom may be further stabilized by the α-helix dipole[15,16]. β-strand 5, the nucleophilic residue, and helix C form the so-called nucleophile elbow, which is the most conserved structure in all α/β hydrolases[5]. Therefore it seems likely that the method of stabilization of the tetrahedral intermediate is the same for all α/β hydrolases, with conservation of the actual mechanism for the hydrolysis of the intermediate ester. In agreement with this is the observation that the interatomic interactions in the active sites are very similar. Dehalogenase extracts a proton from the hydrolytic water molecule at the $N_{\epsilon 2}$ atom of the active-site histidine, while Asp_{260} interacts with the $N_{\delta 1}$ atom of His_{289} through a *syn*-type hydrogen bond. Identical interactions are present in the active sites of dienelactone hydrolase[7], serine carboxypeptidase[9], *Geotrichum candidum* lipase[10] and acetylcholinesterase[6], although these last two enzymes have a glutamic acid interacting with the histidine instead of an aspartic acid residue. Moreover, in the members of the α/β hydrolases with an Asp–His interaction, the plane of the Asp side chain makes an angle of $\sim 45°$ with the plane of the imidazole ring, unlike in the serine proteases, in which the carboxylate side chains are nearly coplanar with the imidazole ring[17,18].

Normally, the lifetime of reaction intermediates in wild-type enzymes is too short for crystallographic observation and millisecond Laue crystallography[19,20] or site-directed mutagenesis[21] have to be used. Here, the combination of low pH and low temperature, and the disparity between alkylation and dealkylation mechanisms in the dehalogenase, with dealkylation as the rate-limiting step under our conditions, allowed us to accumulate different reaction intermediates in the crystals and to analyse these intermediates by conventional protein crystallographic methods. We hope to clarify further details of the reaction mechanism using appropriate mutations. □

Received 1 April; accepted 14 May 1993.

1. Janssen, D. B., Scheper, A., Dijkhuizen, L. & Witholt, B. *Appl. envir. Microbiol.* **49,** 673–677 (1985).
2. Keuning, S., Janssen, D. B. & Witholt, B. *J. Bact.* **163,** 635–639 (1985).
3. Janssen, D. B. *et al. J. Bact.* **171,** 6791–6799 (1989).
4. Franken, S. M., Rozeboom, H. J., Kalk, K. H. & Dijkstra, B. W. *EMBO J.* **10,** 1297–1302 (1991).
5. Ollis, D. L. *et al. Protein Engng* **5,** 197–211 (1992).
6. Sussman, J. L. *et al. Science* **253,** 872–879 (1991).
7. Pathak, D. & Ollis, D. *J. Molec. Biol.* **214,** 497–525 (1990).
8. Liao, D.-I. & Remington, S. J. *J. biol. Chem.* **265,** 6528–6531 (1990).
9. Liao, D.-I., Breddam, K., Sweet, R. M., Bullock, T. & Remington, S. J. *Biochemistry* **31,** 9796–9812 (1992).
10. Schrag, J. D., Li, Y., Wu, S. & Cygler, M. *Nature* **351,** 761–764 (1991).
11. Janssen, D. B. *et al. Eur. J. Biochem.* **171,** 67–72 (1988).
12. Rozeboom, H. J., Kingma, J., Janssen, D. B. & Dijkstra, B. W. *J. molec. Biol.* **200,** 611–612 (1988).
13. Froede, H. C. & Wilson, I. B. *J. biol. Chem.* **259,** 11010–11013 (1984).
14. Douglas, K. T., Nakagawa, Y. & Kaiser, E. T. *J. Am. chem. Soc.* **98,** 8231–8236 (1976).
15. Hol, W. G. J., van Duijnen, P. T. & Berendsen, H. J. C. *Nature* **273,** 443–446 (1978).
16. Hol. W. G. J. *Prog. Biophys. molec.. Biol.* **45,** 149–195 (1985).
17. Kraut, J. *A. Rev. Biochem.* **46,** 331–358 (1977).
18. McPhalen, C. A. & James, M. N. G. *Biochemistry* **27,** 6582–6598 (1988).
19. Hajdu, J. *et al. Nature* **329,** 178–181 (1987).
20. Singer, P. T., Smalas, A., Carty, R. P., Mangel, W. F. & Sweet, R. M. *Science* **259,** 669–673 (1993).
21. Strynadka, N. C. J. *et al. Nature* **359,** 700–705 (1992).
22. Messerschmidt, A. & Pflugrath, J. W. *J. appl. Crystallogr.* **20,** 306–315 (1987).
23. Kabsch, W. *J. appl. Crystallogr.* **21,** 916–924 (1988).
24. Hamilton, W. C., Rollet, J. S. & Sparks, R. A. *Acta crystallogr.* **18,** 129–130 (1965).
25. Read, R. *Acta crystallogr.* **A42,** 140–149 (1986).
26. Tronrud, D. E., ten Eyk, L. F. & Matthews, B. W. *Acta crystallogr.* **A43,** 489–501 (1987).
27. Verschueren, K. H. G., Franken, S. M., Rozeboom, H. J., Kalk, K. H. & Dijkstra, B. W. *J. molec. Biol.* (in the press).

ACKNOWLEDGEMENTS. We thank D. B. Janssen and co-workers for discussion and for the purified protein material, and J. B. F. N. Engberts for advice on Fig. 4.